ELSEVIER

Polymer 42 (2001) 4289–4297

polymer

www.elsevier.nl/locate/polymer

A solid-state ^{13}C NMR study on phase heterogeneity in the miscible blend of amorphous poly(benzyl methacrylate) with semicrystalline poly(ethylene oxide)

Rong-Hsien Lin[a,*], E.M. Woo[b], Jin C. Chiang[b]

[a]*Department of Chemical Engineering, National Kaohsiung Institute of Technology, Kaohsiung 807-82, Taiwan, ROC*
[b]*Department of Chemical Engineering, National Cheng Kung University, Tainan 701-01, Taiwan, ROC*

Received 12 June 2000; received in revised form 2 August 2000; accepted 1 September 2000

Abstract

The rotating-frame spin–lattice relaxation time for protons, $T_{1\rho}(^1H)$, was measured indirectly from ^{13}C CP/MAS/DD NMR to probe possible molecular scales of heterogeneity in the miscible poly(benzyl methacrylate) (PBzMA)/poly(ethylene oxide) (PEO) blend over the whole composition range. According to the NMR results, only one phase was observed for the blends in which the PEO component is less than 16% (w/w). This miscible amorphous phase with PBzMA and PEO chains was mixed at the molecular level. Three phases were detected for the blends with PEO component >16%, containing one miscible homogenous PBzMA-rich phase, one constrained PEO phase and one crystalline PEO phase. The PEO component asymptotically increases in the miscible homogenous PBzMA-rich phase as the PEO composition increases. NMR analysis helped resolve the complex phase domains in the PBzMA/PEO blend that is composed of an amorphous mixture of PBzMA/PEO and crystalline PEO spherulite regions. The intra- and inter-lamellar domains in the PEO spherulites are influenced and complicated by the surrounding amorphous PBzMA/PEO mixture with varying composition.

Keywords: Poly(benzyl methacrylate)/poly(ethylene oxide) blends; NMR; Phase heterogeneity

1. Introduction

Solid-state nuclear magnetic resonance (NMR) is a powerful technique that has been utilized in analyzing miscibility, phase structure or heterogeneity in polymer mixtures. It is especially useful in polymer blend systems containing complex phase structures that may be beyond the resolution limits of conventional microscopic or thermal analysis. An interesting example is seen in the blend system of bisphenol-A polycarbonate (PC) with PMMA, which exhibits a complex phase behavior and dependence of heterogeneity on casting, temperature or annealing. Asano et al. [1] have successfully utilized solid-state NMR to analyze various heterogeneity scales in this blend system. Similarly, the NMR technique has been used in interpreting the compositional dependence of miscibility and phase structure in blends of poly(vinylphenol) with poly(ethylene oxide) (PEO), leading to the conclusion that miscibility is limited to above the 20–30 nm scale [2].

Polymer blends comprising an acrylate and an ether-polymer have attracted extensive studies. A classical miscible blend system is PEO/PMMA, which is a complex system containing semicrystalline PEO and amorphous PMMA components. The phase behavior of this blend system has been extensively investigated by means of differential scanning calorimetry (DSC) [3–5], small-angle X-ray scattering (SAXS) [6], and Fourier-transform infrared spectroscopy (FT-IR) [7–8]. Only a few investigations on PEO/PMMA blends have been performed with nuclear magnetic resonance (NMR) solid-state spectroscopy [9–11]. Parizel et al. [10] investigated PEO/PMMA blends over the whole composition range using ^1H spin–lattice relaxation times in the rotating and laboratory frames. The compositions of each phase were determined by combining ^1H and ^{13}C NMR methods. The organization of the PEO/PMMA blend consisted of three parts: a crystalline PEO, constrained PEO units in the neighborhood of the crystalline lamellae and a miscible amorphous phase that is PMMA-rich. This miscible amorphous phase with PMMA and PEO chains was mixed at the molecular level.

In heterogenous materials, the spin–lattice relaxation

* Corresponding author. Fax: +886-7-7459386.
E-mail address: rongh@ms19.hinet.net (R.-H. Lin).

0032-3861/01/$ - see front matter
PII: S0032-3861(00)00671-6

times in the rotating ($T_{1\rho}(^1H)$) and laboratory frames ($T_1(^1H)$) obtained from high-resolution solid-state ^{13}C CP/MAS/DD (cross-polarization, magic angle spinning, dipolar decoupling) NMR are very sensitive to the size of the domain, which makes them powerful tools for studying miscibility. In recent years, the techniques of measuring $T_{1\rho}(^1H)$ and $T_1(^1H)$ were widely used to investigate the miscibility, micro heterogenous domain size and/or phase structure in various blends [1,2,9–18]. Furthermore, it is possible to quantify the scale of heterogeneities through the spin-diffusion process [1,16]. The measurement of spin–lattice relaxation times permits analysis of domain sizes from a few angstrom to a few tens of nanometers [19,20], depending on the use of $T_{1\rho}(^1H)$ or $T_1(^1H)$.

Another interesting blend system that is an ideal model for solid-state NMR studies is the recently discovered miscible poly(benzyl methacrylate) (PBzMA)/PEO blend [21]. The PBzMA/PEO blend is another example of a blend containing both a semicrystalline (PEO) and an amorphous (PBzMA) component. This blend was found to be miscible judging from the DSC and morphological results [21]. In this continuing study, focus was placed on probing the phase homogeneity and morphologies in the miscible PBzMA/PEO blend comparing the analyses of high-resolution solid-state ^{13}C CP/MAS/DD NMR with the DSC results over the whole composition range.

2. Experimental

2.1. Materials and sample preparation

PEO was purchased from Aldrich Chem. Co. (MW = 200,000 g/mol, $T_g = -65°C$). PBzMA was supplied by Scientific Polymer Products (MW = 70,000 g/mol, $T_g = 56°C$) The molecular weights are the supplier's data as determined by gel permeation chromatograph (GPC). The PEO and PBzMA were used without further purification.

PBzMA/PEO blends were obtained by dissolving the polymers in benzene (approximately 2 g of sample in 100 ml of benzene) at the desired composition. Subsequently, the resulting polymer solution was poured into an aluminum mold kept at the casting temperature of 50°C. The solvent in the cast film samples was first vaporized under a hood at controlled temperature, followed by residual solvent removal in a vacuum oven for 48 days at 80°C to ensure complete removal of benzene solvent. These blend film samples were prepared by solvent-casting at the proper temperature (ca. 50–60°C), which is the lowest temperature chosen to make a visually clear film. Casting of sample films at room temperature (25–30°C) usually led to crystallization of PEO and haziness in the samples. Note that the maximum casting temperature was limited to the boiling temperature of the solvent used.

2.2. Apparatus

2.2.1. Nuclear magnetic resonance

High-resolution solid-state ^{13}C NMR experiments using proton dipolar decoupling (DD), magic angle spinning (MAS) and cross-polarization (CP) were conducted at 9.4 T of magnetic field strength with a Bruker Avance 400 spectrometer. The rotating-frame spin–lattice relaxation time for protons, $T_{1\rho}(^1H)$, was measured indirectly from CP/MAS/DD ^{13}C NMR to achieve a higher spectral resolution. The experimental scheme with a variable spin-lock time after the proton signal excitation followed by constant contact time was used. The contact time was set to 1 ms (for the amorphous case) or 0.1 ms (for the crystalline part). Experiments were performed on magic angle spinning samples contained in rotors. The magic angle (θ) was set to 54.7°, and the spinning speed of the rotors was of the order of 10 kHz. 400 spectra were accumulated. It must be noted that the rotor spinning speed needs to be properly set. Low spinning speeds will result in overlapping between the spinning side-band of carbon atoms in the phenyl ring and the bands of carbon atoms in the other functional group, thereby increasing the difficulty of analysis.

The laboratory-frame spin–lattice relaxation time for protons, $T_1(^1H)$, was measured from CP/MAS/DD ^{13}C NMR using the classical inversion-recovery ($180-\tau-90°$) pulse sequence. The experimental scheme with a variable delay time (τ) after the proton signal excitation followed by constant contact time (1 ms) was used. Two spinning speeds of 10 and 4 kHz were used for comparison. In these experiments, the ^1H magnetization after inversion-recovery was first transferred to ^{13}C and then the resulting ^{13}C signal was acquired. The intensity of ^{13}C resonance as a function of ^1H recovery time provides the T_1 measurement for protons in the blends.

2.2.2. Differential scanning calorimetry (DSC)

A Perkin Elmer DSC-7 instrument was used with an intracooler, which was routinely calibrated with Indium (In) and ethyl acetate (two-point calibration method). A stream of high-purity nitrogen at a flow rate of 20 ml/min was used to purge the DSC cell. The degree of crystallinity (crystalline PEO in the blend) and glass transition temperature (T_g) of the blends were determined by DSC at a heating rate of 10°C/min. The degree of crystallinity is defined as the value of $\Delta H/\Delta H^o_{(PEO)}$, where ΔH refers to the enthalpy of melting per gram of the blend or neat PEO, and $\Delta H^o_{(PEO)}$ is the theoretical enthalpy for perfect crystals of PEO (equal to 205 J/g) [22]. T_g was taken as the temperature at the midpoint of the transition in the DSC trace.

3. Results and discussion

The ^{13}C CP/MAS/DD NMR spectrum of the PBzMA/PEO blend in the 80/20 composition is shown in Fig. 1.

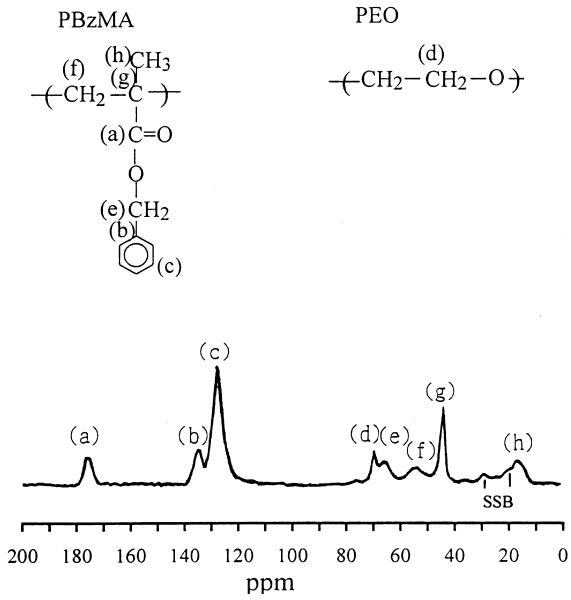

Fig. 1. ^{13}C CP/MAS/DD NMR spectrum of the PBzMA/PEO blend in 80/20 composition. SSB denotes spinning side-band.

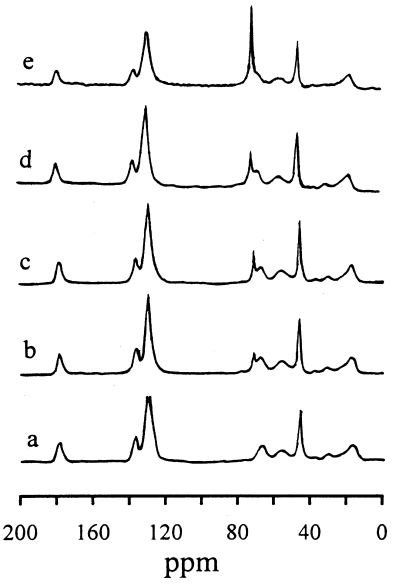

Fig. 2. ^{13}C CP/MAS/DD NMR spectra of the PBzMA/PEO blends in various compositions: (a) 100/0, (b) 90/10, (c) 80/20, (d) 50/50 and (e) 30/70.

The corresponding resonance peaks are assigned to specified carbons indicated in the inset structures. In addition, all assignments of the resonance peaks [23] are summarized in Table 1. The peak at 70 ppm is assigned to the PEO component, while the peaks at 176, 135, 128 and 45 ppm are assigned to the PBzMA component. These peaks were employed in determining the spin–lattice relaxation time, $T_{1\rho}(^1\mathrm{H})$. It should be pointed out that the peak at 27 ppm (denoted as SSB in Fig. 1) is the spinning side-band of a quaternary carbon in the phenyl ring when ^{13}C CP/MAS/DD NMR was carried out. Another spinning side-band of a protonated aromatic-C at 20 ppm was also found overlapping with the peak of carbon in α-CH_3 (16 ppm).

The ^{13}C NMR spectra of various compositions are shown in Fig. 2. The carbonyl peak (176 ppm) in the various compositions did not shift obviously as compared with that peak of neat PBzMA, indicating that the interactions between PEO and PBzMA molecules are rather weak. $T_{1\rho}(^1\mathrm{H})$ relaxation behavior was determined to probe the miscibility of PBzMA/PEO blends because it offers a probe of heterogeneity on a smaller scale than does $T_1(^1\mathrm{H})$ relaxation. A few $T_1(^1\mathrm{H})$ measurements were also performed to explore the domain sizes of the blends.

Table 1
Assignments for chemical shifts in the blend of PBzMA and PEO in the solid-state ^{13}C NMR spectrum

Assignment	Chemical shift (ppm)	Carbon
a	176	carbonyl
b	135	quaternary ring
c	128	protonated ring
d	70	–O–CH_2–(PEO)
e	66	–O–CH_2–(PBzMA)
f	55	–CH_2–
g	45	quaternary carbon
h	16	α-CH_3

3.1. Measurement of $T_{1\rho}(^1H)$ for individual components

The $T_{1\rho}(^1\mathrm{H})$ values can be determined by monitoring the decay of peak intensities using the characteristic assignments in a series of spectra obtained by varying the spin-lock time (t). Because the $T_{1\rho}(^1\mathrm{H})$ relaxation process follows the exponential function $\ln[M(t)/M_{\max}] = -t/T_{1\rho}$, where $M_{\max}$ is the maximum magnetization, the $T_{1\rho}(^1\mathrm{H})$ values were obtained from the slopes in the plots of logarithmic $[M(t)]/M_{\max}]$ against t.

Shown in Fig. 3 are the logarithmic plots of ^{13}C magnetization intensity versus spin-lock time using a 1 ms contact time for neat samples of PBzMA and PEO. Neat PBzMA is characterized by single-exponential $T_{1\rho}(^1\mathrm{H})$ relaxation behavior, consistent with results usually observed on the amorphous polymer. Neat PEO also exhibits a single-exponential $T_{1\rho}(^1\mathrm{H})$ relaxation behavior if using a 1 ms contact time. However, it displays double-exponential $T_{1\rho}(^1\mathrm{H})$ relaxation behavior if using a 0.1 ms contact time, indicating that PEO contains dual morphologies. Essentially, PEO is a well-known semicrystalline polymer containing an amorphous phase and a crystalline phase. It should be noted that crystalline PEO, which has a very short $T_{1\rho}(^1\mathrm{H})$, cannot be detected using a 1 ms contact time. The fitted values of $T_{1\rho}(^1\mathrm{H})$ are 7.74 ms for neat PbzMA, and 2.72 and 0.2 ms for neat PEO, as listed in Table 2. According to the literature [13], the short $T_{1\rho}(^1\mathrm{H})$ (0.2 ms) can be associated with the protons of the crystalline parts of PEO,

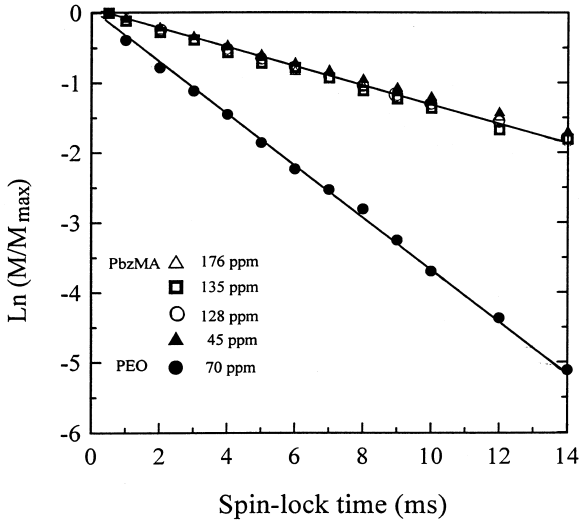

Fig. 3. $T_{1\rho}(^1H)$ decays obtained in the nuclei of (a) neat PBzMA and (b) neat PEO, contact time = 1 ms.

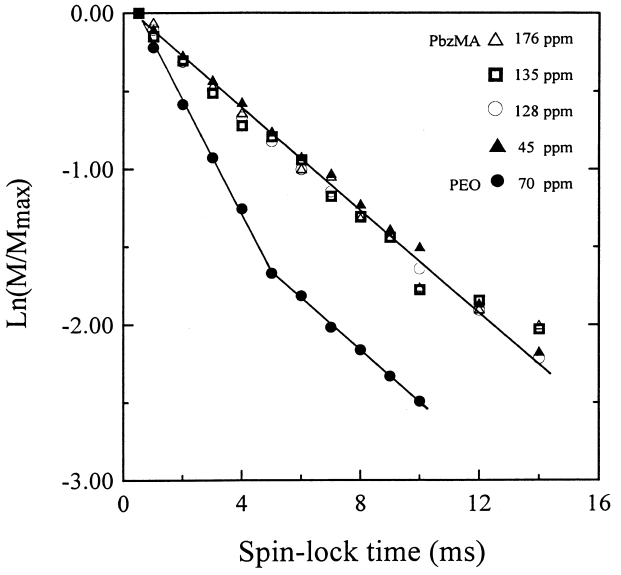

Fig. 4. $T_{1\rho}(^1H)$ decays obtained in the PBzMA/PEO (80/20) blend, contact time = 1 ms.

and long $T_{1\rho}(^1H)$ (2.72 ms) is contributed by the amorphous phase of PEO.

The degree of crystallinity in neat PEO was calculated from the enthalpy of melting (ΔH) obtained from DSC thermograms, and a value of 75% (w/w) was obtained. It should be noted that the degree of crystallinity obtained from DSC may be slightly underestimated compared with that from $T_{1\rho}(^1H)$ relaxation, probably because some tiny crystals (<10 nm) are below the detection threshold of DSC.

3.2. Measurement of $T_{1\rho}(^1H)$

Fig. 4 shows the logarithmic plot of ^{13}C magnetization intensity versus spin-lock time using a 1 ms contact time for as-cast samples of PBzMA/PEO blend in the 80/20 composition. The logarithmic plots of ^{13}C magnetization intensity versus spin-lock time for the other composition (90/10, 50/50 and 30/70) are not shown here for brevity. The fitted values of $T_{1\rho}(^1H)$ are summarized in Table 2. PBzMA components in the blends were observed to exhibit single-exponential $T_{1\rho}(^1H)$ relaxation behavior through all the cases of different compositions, indicating that the PBzMA component always exhibits a homogenous phase within the blends at various compositions. This homogenous phase is not pure PBzMA, because the values of $T_{1\rho}(^1H)$ for the PBzMA component are not identical to that in the neat PBzMA system (7.74 ms). In spite of the PEO content in the blend, the PBzMA component always predominates in the miscible amorphous phase because the $T_{1\rho}(^1H)$ values in this phase are always closer to that of the neat PBzMA component (7.74 ms) and far way from that of the neat amorphous PEO component (2.72 ms). That indicates a miscible homogenous PBzMA-rich phase at a nanoscale level in the blends. Besides, those values of $T_{1\rho}(^1H)$ for the PBzMA component slightly decrease (approaching the value of neat PEO) as the PEO component in the blend increases, suggesting that the PEO component in this miscible homogenous phase is presumably enhanced in a gradual way. Another possibility for the reduction in the $T_{1\rho}(^1H)$ of this miscible homogenous phase is that there is a very modest spin diffusion contribution from the amorphous PEO phase, but it is not so for this case because the same

Table 2
$T_{1\rho}(^1H)$ relaxation times for the neat PBzMA, neat PEO, and respective constituent polymers in PBzMA/PEO blends of several compositions studied (contact time: 1ms)

PBzMA/PEO blend (w/w)	PBzMA component $T_{1\rho}(^1H)$ (ms)	PEO component $T_{1\rho}(^1H)$ (ms)		
100/0	7.74	–		
90/10	6.27	6.33	–	
80/20	6.03	6.02,	2.76	
50/50	5.72	5.70	2.77	
30/70	5.34	5.40	2.73	
0/100	–		2.72	0.2[a]

[a] Obtained using a contact time of 0.1 ms.

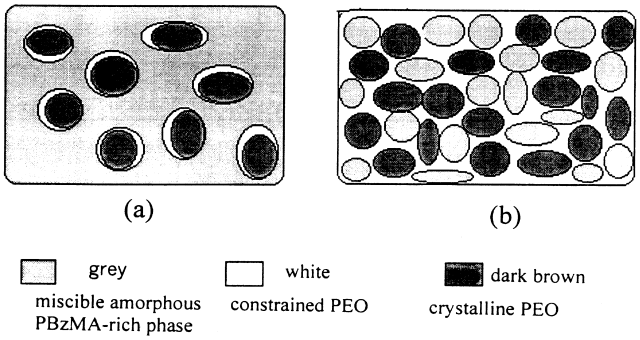

Fig. 5. Proposed schematic morphology illustrated for the PBzMA/PEO blends: (a) for low PEO compositions (but ≥20%) and (b) for high PEO compositions.

spinning frequency was used for various compositions and the high spinning frequency of 10 kHz used may effectively quench spin diffusion between the amorphous PEO and PBzMA phases. Meanwhile, for each blend the $T_{1\rho}(^1H)$ values for PBzMA (6.27, 6.03, 5.72 and 5.34 ms) are eventually identical to the long $T_{1\rho}(^1H)$ of the PEO component. This indicates those miscible homogenous phases with PBzMA and PEO chains mixed at the molecular level.

On the other hand, double-exponential $T_{1\rho}(^1H)$ relaxation behavior of the PEO component in various compositions of blends except 90/10 (PBzMA/PEO) were clearly observed by the slope change in the 70 ppm signal in the logarithmic plot of ^{13}C magnetization intensity. The long $T_{1\rho}(^1H)$ of the PEO component was virtually the same as the $T_{1\rho}(^1H)$ of PBzMA in the PBzMA-rich domain for each composition of blend, whereas all the short $T_{1\rho}(^1H)$s of the PEO component in each blend were of the same value (about 2.75 ms) and identical with that of the amorphous phase of neat PEO. This suggests that the amorphous PEO component in each blend is distributed unevenly into two separated phase domains on a $T_{1\rho}(^1H)$ relaxation scale. These two phase-separated domains are the amorphous PBzMA-rich phase domain with complete homogeneity (hereafter called the miscible homogenous PBzMA-rich phase) and the amorphous PEO-rich phase domain. If this amorphous PEO-rich phase contained the PBzMA component, the value of the short $T_{1\rho}(^1H)$ of the PEO component should lie between 7.74 ms (neat amorphous PBzMA) and 2.70 ms (amorphous PEO). However, the fact that they have the same values of $T_{1\rho}(^1H)$ as the amorphous phase of neat PEO suggests that they do not contain any PBzMA component. If this amorphous phase in neat PEO did contain some 'rigid' PEO units (referred to as the constrained PEO [10]) at the front of the PEO crystals, the value of the short $T_{1\rho}(^1H)$ of the PEO component should lie between those of the amorphous (2.72 ms) and crystalline phases (0.2 ms). In fact, no evidence of the presence of rigid PEO units was found in this amorphous phase of neat PEO (i.e. it is not blended). Nevertheless, this amorphous neat PEO phase is still referred to as the 'constrained PEO', because PEO crystals are typically surrounded by this amorphous PEO; hence, the presence of the embedded PEO crystals provides some constraint for the surrounding amorphous PEO. The crystalline PEO, which has a very short $T_{1\rho}(^1H)$, was not detected using a 1 ms contact time. Usually, the amount of constrained PEO was less than that of crystalline PEO (to be calculated later).

The PEO component in the blend of 90/10 (PBzMA/PEO) composition still exhibits a single-exponential $T_{1\rho}(^1H)$ relaxation behavior (6.33 ms). This single value of $T_{1\rho}(^1H)$ for the PEO component is virtually the same as that of the PBzMA component, indicating that this blend is completely homogenous PBzMA-rich phase without constrained PEO and crystalline PEO. Crystalline PEO usually coexists with constrained PEO, because the crystalline PEO crystallizes out of the originally amorphous PEO domain. Thus, the non-crystallizable portion is referred to the 'constrained PEO' region. This inference illustrates that only one phase is present for this blend (90/10), which will be verified later in more detail.

A morphologic illustration for blends whose PEO component is >20% is drawn and shown in Fig. 5. Fig. 5a illustrates the morphology of the blends with large contents of PBzMA, consisting of a continuous phase of the miscible homogenous PBzMA-rich domain and a dispersed phase in which the crystalline PEO is surrounded by the constrained PEO. Fig. 5b illustrates the schematic morphology of the blends with large contents of PEO, consisting of a continuous phase of amorphous pure PEO (i.e. constrained PEO) and two dispersed phases involving one crystalline PEO phase and one miscible homogenous PBzMA-rich phase. The crystalline PEO in this morphology is, of course, also surrounded by the constrained PEO. In these illustrated morphologies, the PEO component is distributed into three domains: the miscible homogenous PBzMA-rich domain, the constrained PEO domain and the crystalline PEO domain. The crystalline PEO domain forms during crystallizing out of the amorphous pure PEO phase when cooled to room temperature from the casting temperature. It should be mentioned that the domain sizes in this illustrated morphology will be discussed later. We proved the presence of crystalline PEO by simply shortening the CP contact time. Then, it is possible to detect the presence of both crystalline PEO and constrained PEO.

3.3. Evidence of crystalline PEO in various blend compositions

By using the ^{13}C CP/MAS/DD NMR analysis of PEO, Dechter et al. [13] identified two components in the complex ^{13}C peak shape. A narrow component was observed superimposed on a broad component. Fine-tuning the contact time of the rotating-frame can discriminate between the narrow component and the broad component. For short contact times, the superimposed broad and narrow components are obtained, while for long contact time, the narrow component is predominately obtained. Thus, the

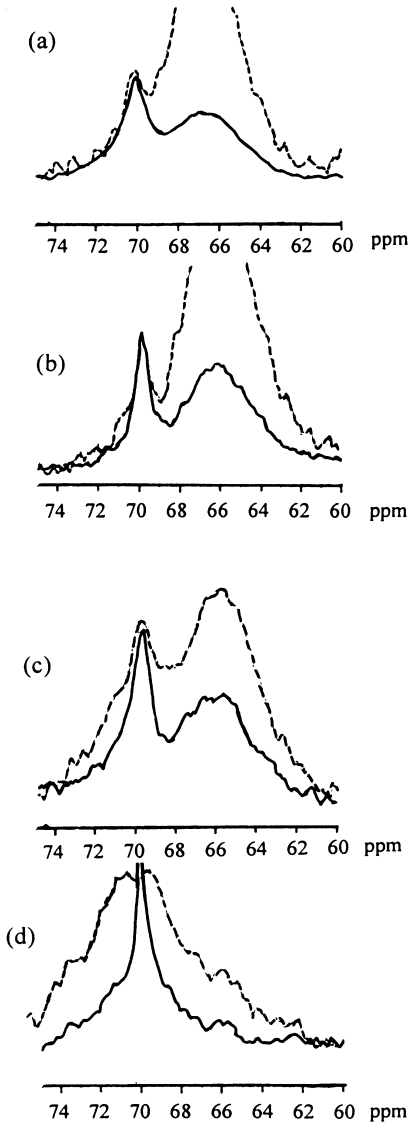

Fig. 6. Effect of contact time on the PEO resonance (70 ppm) in the normalized ^{13}C CP/MAS/DD NMR spectra: (a) blend PBzMA/PEO 90/10, (b) blend PBzMA/PEO 80/20, (c) blend PBzMA/PEO 50/50 and (d) neat PEO (- - -) contact time = 0.1 ms, (—) contact time = 1 ms. (It should be pointed out that the peak of 66 ppm is an assignment of PBzMA.)

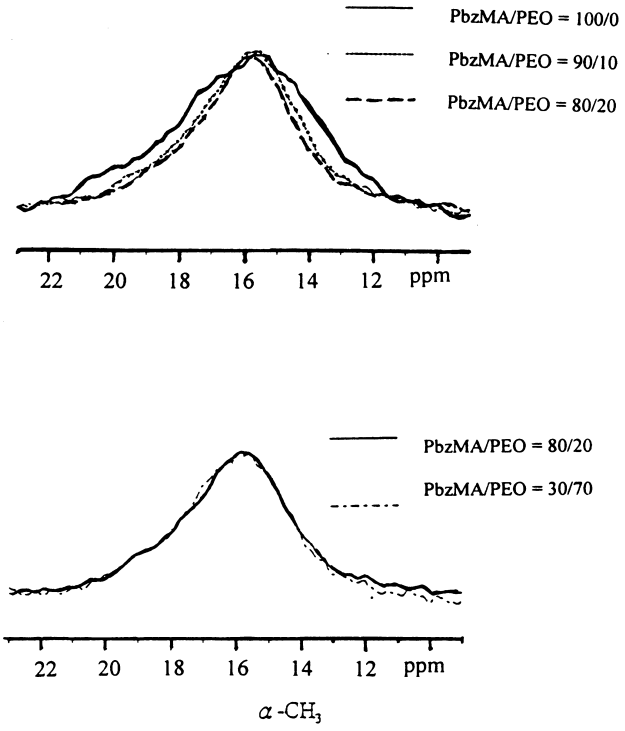

Fig. 7. Chemical shifts of the PBzMA α-CH_3 band in the various compositions of the PBzMA/PEO blend in the ^{13}C CP/MAS/DD NMR spectra.

broad component is associated with a faster rotating-frame relaxation rate (i.e. the short $T_{1\rho}(^1H)$). The short $T_{1\rho}(^1H)$ was further identified with the protons of the crystalline parts of the PEO. Fig. 6 shows the effect of contact time on the characteristic peak shape (70 ppm) for the PEO component in various compositions of PBzMA/PEO blends. The contact times were set at 1 and 0.1 ms, respectively. Using the 0.1 ms contact time of the rotating-frames, a broader superimposed peak was observed in each blend except for the 90/10 and 80/20 blends. It becomes more apparent as the PEO composition in the PBzMA/PEO blend increases. The results demonstrate the existence of crystalline PEO in the blends with PEO contents >20% (presumably aggregating in the constrained PEO domain), and also indicate that the amount of crystalline PEO in the PBzMA/PEO blends increases with the PEO content in the blend. More precisely, the amounts of crystalline PEO and constrained PEO in the PBzMA/PEO blends simultaneously increase as the composition of PEO in the PBzMA/PEO blends increases. This is because the PEO components in the miscible homogenous PBzMA-rich phases are enhanced only a small amount as the composition of PEO in PBzMA/PEO blends increases. This will be further justified by the following calculations.

3.4. Composition of different phases in the PBzMA/PEO blends

Miscibility may enhance or retard polymer backbone mobility in a homogenous phase depending on the interactions between the constituents. Mobility more often broadens CP/MAS peakwidths, especially if there is a contrast between crystalline-rigid and non-crystalline-mobile chains. Mobility for amorphous chains can either broaden or narrow resonances depending on the frequency of motion. A decrease in the composition of PMMA seems to narrow the peakwidth of the α-CH_3 carbon in the PMMA component in the solid ^{13}C CP/MAS/DD NMR spectra of the PMMA/PEO blends [9]. In the solid ^{13}C CP/MAS/DD NMR spectra of the PBzMA/PEO blends, the peakwidths of all the characteristic bands of the PBzMA components became narrower as the PEO composition in the blends increased. Fig. 7 is a representative peak showing the change in peakshape of the α-CH_3 carbon in

Table 3
Composition of the different phases of the PBzMA/PEO semicrystalline blend

PBzMA/PEO blend (%) (w/w)	PBzMA in the blend (%) (w/w)[a]	PEO repartition (%) (w/w)		Degree of crystallinity (%)[b]	Constrained PEO (%) (w/w)
		in miscible phase[a] — (PBzMA-rich domain)	crystalline and constrained		
100/0	100	0	0	0	0
90/10	90 (90.0)	10 (10.0)	0	0	0
80/20	80 (86.5)	12.5 (13.5)	7.5	5.5	2.0
50/50	50 (83.2)	10.1 (16.8)	39.9	30.0	9.9
30/70	30 (79.5)	7.7 (20.5)	62.3	46.8	15.5
0/100	0	0	100	75.0	25.0

[a] Calculated by the Dickinson equation, where PBzMA = 70,000 g/mol; $N_A = 4772.7$ protons for each PBzMA polymer; PEO = 200,000 g/mol; $N_B = 18{,}182$ protons for each PEO polymer. The values within parentheses were based on the total amount of miscible homogenous phase (PBzMA-rich domain). Weight fractions were transferred from the mole fraction calculated from the Dickinson equation.

[b] Degree of crystallinity = $\Delta H/\Delta H^{o}_{(PEO)}$, where ΔH refers to enthalpies of melting per gram of blend or neat PEO; $\Delta H^{o}_{(PEO)} = 205$ J/g, theoretical enthalpy of melting for perfect crystal of PEO.

PBzMA. The largest effect was observed for the peakshape of this carbon due to the fact that it has less steric-hindrance. The peakwidth gradually decreased up to 20% PEO content but at higher PEO content the peakwidth did not further change. This indicates that the PEO component has an asymptotic value in the miscible homogenous PBzMA-rich domain, consistent with the observation in the measurement of $T_{1\rho}(^1H)$ (as previously described) and with the calculated results (as shown later).

The composition of each component in the miscible homogenous PBzMA-rich domain can be quantitatively estimated by the Dickinson equation [24]. In a miscible blend of two polymers A and B, the $T_{1\rho}(^1H)$ of the blend can be written as

$$\frac{1}{T_{1\rho}(^1H)_{AB}} = \left(\frac{N_A M_A}{N T_{1\rho}(^1H)_A}\right) + \left(\frac{N_B M_B}{N T_{1\rho}(^1H)_B}\right)$$

where $T_{1\rho}(^1H)_A$ and $T_{1\rho}(^1H)_B$ refer to the relaxation times of the neat components A and B, M_A and M_B are the molar fractions of each polymer, N_A and N_B are the numbers of protons contained in each polymer, and $N = N_A M_A + N_B M_B$. The relative amounts of PBzMA and PEO in the miscible homogenous PBzMA-rich domain were obtained from the Dickinson equation. The amount of PBzMA in this miscible homogenous PBzMA-rich phase was given due to the fact that the PBzMA components were all distributed in this PBzMA-rich phase. Accordingly, the amount of PEO in this miscible homogenous PBzMA-rich phase can be calculated from the relative amount to PBzMA. Consequently, the amounts of the other phases can be obtained. Results of calculated M_A, M_B and the corresponding weight fractions are given in Table 3. Degrees of crystallinity of the blends were calculated from the enthalpy of melting (ΔH) obtained from DSC thermograms. This table shows the composition of the different phases of the PBzMA/PEO semicrystalline blend. For blends below 20% PEO content (more precisely below 16% or so), the same values of $T_{1\rho}(^1H)$ for the PBzMA and PEO components were obtained, and only one glass-transition temperature and no melting peak was observed on the DSC thermograms; only one phase was present in this region: it is the miscible homogenous PBzMA-rich phase. The PEO component was completely miscible with the PBzMA component at the molecular level. However, when the PEO content is over 16%, three phases containing one miscible homogenous PBzMA-rich phase, one constrained PEO phase and one crystalline PEO phase were found (as proposed in Fig. 5). Two different values of $T_{1\rho}(^1H)$ were measured at the 1 ms contact time. The short $T_{1\rho}(^1H)$ is associated with the protons of the constrained PEO, and the long $T_{1\rho}(^1H)$ (actually two values) is associated with the protons of both components (PEO and PBzMA) in the miscible homogenous PBzMA-rich phase, whereas the crystalline PEO phase was not detected by ^{13}C CP/MAS/DD NMR using a 1 ms contact time of the rotating-frame. The broader peakwidth with the contact time of 0.1 ms and the melting peak on the DSC thermogram provide evidence of the presence of crystalline PEO. From Table 3, it demonstrates that the crystalline PEO is always accompanied by the constrained PEO and that the amount of constrained PEO is always much less than that of crystalline PEO.

The average domain sizes in the linear dimension can be estimated using the formula for the maximum diffusion path length [1,16], $L = (6D\mathrm{Ti})^{1/2}$, where D is the spin-diffusion coefficient and Ti is either $T_{1\rho}(^1H)$ or $T_1(^1H)$ according to the relaxation experiment. The spin-diffusion coefficient D was estimated to have values of the order of 8.0×10^{-16} and 1.0×10^{-16} m^2/s from the PMMA/PS blend [25] and PMMA/PEO blend [9], respectively. Based on analogy to the structure, a value of 1.0×10^{-16} m^2/s is probably a reasonable estimate for the PBzMA/PEO blends. Using the measured $T_{1\rho}(^1H)$ values and the estimated spin-diffusion coefficient $D = 1.0 \times 10^{-16}$ m^2/s we obtained the linear domain sizes $L = 1.8$–2.2 and 1.3 nm for the miscible homogenous PBzMA-rich phase and the constrained PEO phase in the pseudodomain sense, respectively. Since we

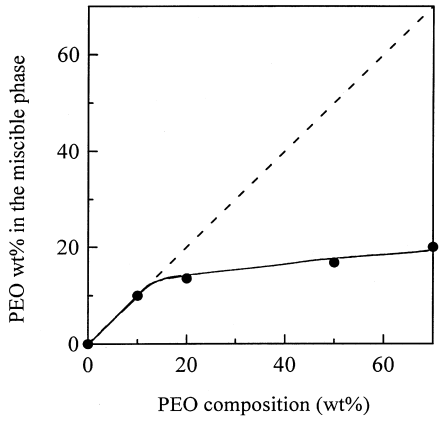

Fig. 8. Change of the actual PEO content in this miscible amorphous phase with the apparent PEO composition in the blends.

have demonstrated no spin diffusion between these two domains, these calculations only present a lower limit on the domain size. Domain sizes may be much larger than these values and could be additionally estimated from the $T_1(^1H)$ values. For the cases using a spinning speed of 10 kHz, the $T_1(^1H)$ values for the PBzMA component and amorphous PEO in the miscible homogenous PBzMA-rich phase lie between 0.15 s (in the 90/10, PBzMA/PEO blend) and 0.31 s (in the 30/70 blend). The $T_1(^1H)$ values for the constrained PEO in the blends are about 0.70 s. Using the measured $T_1(^1H)$ values and the estimated spin-diffusion coefficient, we obtained the maximum average sizes of PBzMA-rich domain as 9.5–14 nm and the constrained PEO domain size as 20 nm. The $T_1(^1H)$ values for each phase increased by 0.9–13% when using a spinning speed of 4 kHz. Consequently, the estimated maximum average sizes for each phase correspondingly increased by 4.5–6.5%.

The results of $T_{1\rho}(^1H)$ and $T_1(^1H)$ experiments demonstrated that the domain sizes were all in the range of a few tens of nanometers. ^{13}C CP/MAS/DD NMR can discriminate between the miscible homogenous PBzMA-rich phase and the constrained PEO phase in these ranges of domain sizes, while DSC analysis cannot tell the difference in phases (only one T_g obtained), presumably because the domain sizes or amounts of the constrained PEO are too small and below the detection threshold of DSC.

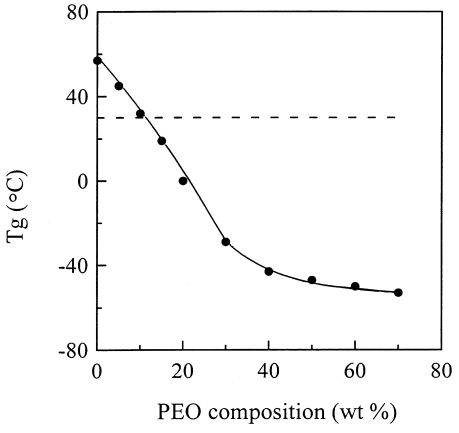

Fig. 9. Change of T_g of the blends with the apparent composition of PEO in the blends.

Variation of the actual PEO content in the miscible homogenous PBzMA-rich phase with the apparent PEO composition in the blends is shown in Fig. 8. This illustrates that the PEO component has an asymptotic value in the miscible homogenous PBzMA-rich domain, consistent with the observation in the changes in the peakwidth of the PBzMA α-CH_3 carbon. The PEO component in the miscible amorphous phase sharply increased up to 16% PEO content, and gradually leveled off beyond 20% PEO content. This may be related to the difference between the glass-transition temperature (T_g) of each blend and the crystallization temperature of PEO (30°C).

Fig. 9 shows the change of T_g of the blends with the composition of PEO. The T_gs of the blends with less than 10% PEO content were higher than the crystallization temperature of PEO (30°C). In this case, the polymer chains of the PEO component are not mobile enough to fold to form lamellae crystals. That is why they appear in an amorphous state and subsequently merge homogenously in the domain of the PBzMA component. At higher PEO composition, the blend T_g becomes much lower than 30°C, which provides a mechanism to pack into crystals from a kinetic point of view. From a thermodynamic view, it is also of interest to note that the relative amount of crystalline PEO versus constrained PEO depends on the annealing time at room temperature. It is supposed that the blend sample annealed at room temperature for 4 days has reached thermodynamic equilibrium between the amorphous and crystalline domains. The calculated amounts of crystalline PEO shown in Table 3 are for the blends reaching a thermodynamic equilibrium. These calculated results exhibit that the amount of crystalline PEO increases with increasing PEO composition in the blend. Within the experimental uncertainty of T_g, the critical composition for forming crystalline PEO from a mixed phase whose $T_g < 30$°C lies in the vicinity of 16% PEO content (as shown in Fig. 9), consistent with all observations as previously mentioned.

4. Conclusions

Although it has been earlier determined that some PBzMA/PEO blends are miscible in the amorphous domain, the various scales of heterogeneity in the amorphous domain as well as in the crystalline domains have yet to be understood. The spin–lattice relaxation times in the rotating ($T_{1\rho}(^1H)$) obtained from high-resolution solid-state CP/MAS/DD ^{13}C NMR can further discriminate the constrained PEO phase from the miscible homogenous PBzMA-rich phase in this amorphous domain.

Only one phase was observed for the blend containing a

PEO component <16%, whereas three phases were detected for the blends whose PEO fraction was >16%, containing one miscible homogenous PBzMA-rich phase, one constraint PEO phase and one crystalline PEO phase. $T_{1\rho}(^1H)$ values have been interpreted in terms of varying composition in the different phases of the PBzMA/PEO blends; moreover a morphologic picture for the three-phased blends was proposed. This morphology is somewhat like the PMMA/PEO system described by Parizel et al. [10], probably due to the similarity in the PMMA and PBzMA structure.

The PEO component has an asymptotic value in the miscible homogenous PBzMA-rich domain in the PBzMA/PEO blend. We speculate that different miscible blends containing a PEO component have different asymptotic values, presumably due to relatively low crystallization temperature and the relative ease of PEO crystallization in the blend and/or different interaction strength. In this three-phase case, the PEO component is distributed into the miscible homogenous phase, the constrained PEO phase, and the crystalline PEO phase. The amount of crystalline PEO in such blends depends on whether or not the blend has reached thermodynamic equilibrium.

Acknowledgements

Research grant (#NSC 87-2216-E006-005) for this study was provided by National Science Council of Taiwan. The authors are grateful for the NMR technical assistance provided by Ms. R.R. Wu of Regional Analytical Instrument Center administered by the National Science Council.

References

[1] Asano A, Takegoshi K, Hikichi K. Polym J 1992;24:555.
[2] Zhang X, Takegoshi K, Hikichi K. Macromolecules 1992;25:2336.
[3] Silvestre C, Cimmino S, Martuscelli E, Karasz FE, McKnight WJ. Polymer 1987;28:1190.
[4] Zawada JA, Ylitalo CM, Fuller GG, Colby RH, Long TE. Macromolecules 1992;25:2896.
[5] Liberman SA, Gomes A, De S. J Polym Sci, Part A: Polym Chem 1984;22:2809.
[6] Russel TP, Ito H, Wignal GD. Macromolecules 1988;21:1703.
[7] Marcos J, Orlandi E, Zerbi G. Polymer 1990;31:1899.
[8] Makhija S, Pearce EM, Kwei TK. J Polym Sci, Part A: Polym Chem 1992;30:2693.
[9] Straka J, Schmidt P, Dybal J, Schneider B, Spevacek J. Polymer 1995;36:1147.
[10] Parizel N, Laupretre F, Monnerie L. Polymer 1997;38:3719.
[11] Brosseau C, Guillermo A, Cohen-Addad JP. Polymer 1992;33:2076.
[12] Tekely P, Laupretre F, Monnerie. Polymer 1985;26:1081.
[13] Dechter JJ. J Polym Sci, Polym Lett Ed 1985;23:261.
[14] Parmer JF, Dickinson LC, Chien JCW, Porter RS. Macromolecules 1989;22:1078.
[15] Tang P, Reimer JA, Denn MM. Macromolecules 1993;26:4269.
[16] Kwak SY, Nakajima N. Macromolecules 1996;29:3521.
[17] Kwak SY, Nakajima N. Macromolecules 1996;29:5446.
[18] Grobelny J. Polymer 1999;40:2939.
[19] Masson JF, Manley RStJ. Macromolecules 1991;24:6670.
[20] Komoroski RA. High resolution NMR spectroscopy of synthetic polymer in bulk. New York: VCH, 1986.
[21] Mandal TK, Kuo JF, Woo EM. J Polym Sci, Polym Phys Ed 2000;38:562.
[22] Martuscelli E, Silvestre C, Addonizio ML, Amelino L. Makromol Chem 1986;187:1557.
[23] Pretsch E, Clerc T, Seibl J, Simon W. Tables of spectral data for structure determination of organic compounds. 2. Berlin: Springer, 1989.
[24] Dickinson LC, Yang H, Chu CW, Stein RS, Chien JCW. Macromolecules 1987;20:1757.
[25] Clauss J, Schmidt-Rohr K, Spiess HW. Acta Polym 1993;44:1.